FLOYD M. HENDERSON
Department of Geography
State University of New York at Albany
Albany, NY 12222

A Comparison of SAR Brightness Levels and Urban Land-Cover Classes

Urban and non-urban land cover was mapped and land-cover type examined in terms of the homogeneity and heterogeneity of its SAR signal response.

INTRODUCTION

THE INCREASED AVAILABILITY of radar imagery, particularly digitally processed space imaging synthetic aperture radar (SAR) systems, has focused attention on the necessity of more precisely defining and understanding the radar signal/target relationship for a broad range of applications. Moreover, such effort is paramount given the interest in de-

In previous work digitally processed Seasat SAR imagery of Denver, Colorado (Henderson and Wharton, 1980) was examined. Among the conclusions were that (1) the urban/non-urban boundary as well as land cover at a modified Level II detail could be delimited using a piecewise linear contrast stretch image of the raw data; (2) interpretation accuracies for large and intermediate scale imagery

ABSTRACT: *A digitally processed Seasat* SAR *(L-band) scene of Harrisburg, Pennsylvania is examined using linear contrast stretch, window-averaging filters, image enlargements, and iterative density level slicing techniques. A total of 33 images were generated and interpreted by manual and semi-automated procedures. In addition to discriminating urban versus non-urban land cover, each land-cover type was examined in terms of the homogeneity and heterogeneity of its* SAR *signal response. The most accurate results were attained with a black-and-white maximum enlargement image that had been subjected to linear contrast stretch (83.1 percent accuracy). Little correlation was found between a land-cover class and its* SAR *signal response pattern. Each iterative response level contained diverse land-cover types and, conversely, each land-cover type was characterized by range of brightness (density) levels. An explanation involves a combination of environmental and radar system parameters. The merits of using both tone and texture information and the complex nature of the radar signal/urban terrain response relationship continue to point to human/manual image analysis.*

veloping semi-automated remote sensing interpretation techniques *per se* as well as determining the role of SAR data as a component in merged data sets. The purpose of this study is to explore the utility of digitally processed SAR imagery for urban land-cover mapping by examining (1) the effects of selected filtering and averaging techniques and (2) the agreement between urban land-cover classes and SAR signal return as expressed by brightness levels.

enlargements were comparable; and (3) density slicing and color coding the imagery was of little if any value. However, in order to evaluate the consistency of these results, additional work was recommended using urban areas in other environments and additional preprocessing techniques.

In a continuation of this effort, Wharton and Henderson (1982) conducted a preliminary analysis of Seasat SAR imagery of the Harrisburg, Pennsylvania,

area. Among their conclusions were that environment and urban morphology did affect interpretability. For the Harrisburg area it was not possible to interpret land cover by type, and even urban/non-urban discrimination was difficult. While contrast stretch did improve interpretation, the results were inconsistent for the 15 image generations examined. Moreover, a higher accuracy was attained with the large scale imagery. Last, they found that color-coded density sliced imagery was inferior to black-and-white imagery.

This study employed the same digitally processed Seasat SAR (L-Band) image of Harrisburg, Pennsylvania, obtained on ascending pass 1296, 25 September 1978. The purpose was to examine the relationship between urban land-cover categories and SAR brightness levels as expressed by density slices. Thirty-three image generations were employed in an expanded test of urban land-cover mapping potential. Land cover was defined as urban by an incremental stepped procedure to determine the accuracy attained by varying the urban/non-urban breakpoint among the level slices. Second, the composition of residential land-cover categories and brightness levels (density slices) was examined for each of the six filtered images. That is, the number and proportion of each land-cover type within each level slice was calculated to obtain a measure of the homogeneity/heterogeneity of that brightness range. Conversely, the homogeneity of each land-cover type's signal response was determined by calculating the proportion of each brightness range within each land-cover category.

METHODOLOGY AND ANALYSIS

The Harrisburg SAR scene was analyzed at two scales, 1:51,000 and 1:145,000. The former was the maximum enlargement possible without resampling the data. The latter scale was selected for analysis based on the earlier Denver work (Henderson, 1980).

At each scale two approaches were employed—a visual interpretation of the black-and-white image and a semi-automated machine/visual interpretation (i.e., generation of land-cover classes by density slicing the image gray levels, assigning colors to the classes, and visual interpretation of the color image).

The imagery was generated using the NASA Goddard Space Flight Center's Electromagnetic Systems Laboratory (ESL) IDIMS digital image analysis system. In addition to the raw data imagery, piecewise linear contrast stretch was applied to the appropriate subset of each image. Smoothing was performed by using a 3 by 3, 5 by 5, and 7 by 7 pixel filter and the ESL IDIMS (ESL, 1980) convolution function. Positive prints of each data set were produced for subsequent visual/manual interpretation. Initial attempts to discriminate Level II land-cover detail were unsuccessful (Wharton and Henderson, 1982). The decision was then made to define the urban fringe by using only two classes of land cover: urban and non-urban. The stretched data and each window-averaged scene at both scales were sliced and color-coded by an iterative process (Henderson and Wharton, 1980). Break points in the histograms were selected, and the resulting classes were defined in terms of known land-cover patterns and the observed spatial distribution of SAR signal response patterns.

Each of the filtered, density sliced scenes was then partitioned into seven color-coded classes, and the urban/non-urban land cover was defined by visual/manual interpretation. Next, only the iteratively-derived break points were used to classify land cover. That is, land cover was defined as urban or non-urban solely on the basis of its response level (color) to determine the merit of such an objective, automated approach. The two highest and two lowest level slices were defined as urban and nonurban, respectively. The intervening colors (level slices), to a greater or lesser extent, contained both land-cover types. By adding each of these three levels consecutively to the urban class and calculating the resulting accuracy, an estimate of semiautomated urban land-cover detectability was attained for four breakpoints, two scales, and three filters. The procedure also provided some indication of the relationship among land cover, SAR brightness response, and texture as represented by filtering.

The last part of the study used each of the color-coded density sliced images to determine the mix of land cover found in each density slice. For this step Level II land-cover classes (Anderson et al., 1976) were employed. Ground data used for comparison with the SAR data to establish accuracy consisted of 1972 USGS land-use maps updated with contemporary (1978) black-and-white and color infrared aerial photography and an on-site visit. For each data set the color-coded SAR image was placed over the revised ground data land-use map, and a contingency table was generated using a grid representing 4-acre units on the ground and a systematic unaligned sampling technique. In each instance the entire study area was classified. In deriving errors of omission and commission for each phase or approach and SAR image, the following equations (after Estes and Senger, 1971) were used:

$$\% \text{ Omission} = 100\% - \left(\frac{\text{\# of cells classified into a category}}{\text{total actual cells in that category}} \times 100 \right)$$

$$\% \text{ Commission} = \frac{\text{total number of commission errors for a category}}{\text{total possible responses} - \text{total possible correct responses for a category}} \times 100$$

RESULTS AND DISCUSSION

For brevity, the following terms will be used in discussing the respective image scenes: CITY = large scale (1:51,000) image scene enlargements; OVW = small scale (1:145,000) overview SAR scene enlargements of the urban area; COLOR = color coded density sliced scenes; 3 × 3, 5 × 5, etc. = pixel filter scenes.

The interpretation errors and accuracies attained in discriminating urban from non-urban land cover for the black-and-white scenes generated at two scales with the selected pre-processing algorithms have been reported earlier in Wharton and Henderson (1982). For comparative purposes, a brief summary is in order. At the CITY scale the highest accuracy was achieved with the data that had been piecewise linear stretched (83.1 percent) while the raw SAR data scene produced the poorest results (45.1 percent). An examination of the raw data OVW scene indicated that interpretation would be of little value due to excessive speckle; it was omitted from further study. As a rule, none of the smaller scale (OVW) scenes was as accurate as the CITY scenes. Also, the OVW stretched data were not the most accurate, a position now assumed by the 5 by 5 filtered scene.

At the smaller (OVW) scale, instances of high return erroneously designated as urban land cover were actually groups of farm buildings, stream banks, tree lines, and other non-urban features with corner-reflector or other high return properties also characteristic of urban land cover. These non-urban cover types appeared to be outliers of urban activity on the urban fringe. This fact may explain why the filtered scenes proved better than the stretched scene at this scale because many of these isolated high returns were lost when the pixels were averaged and filtered. That is, texture and speckle variations that contributed to confusion and uncertainty to the interpretation were lessened by the smoothing process inherent in the filter algorithm.

COLOR: The results of the visually interpreted color scenes and break-point derived color classification can be seen in Table 1. At the CITY scale there was no significant difference among the three COLOR pixel scenes that were visually interpreted. An accuracy of around 70 percent was attained for each with similar errors of omission and commission. At the smaller OVW COLOR scale, however, the 7 by 7 COLOR filter proved the most accurate (68.2 percent). This scene produced the most general view of the urban area by averaging out instances of small, isolated high return that were erroneously interpreted as urban land cover on the 3 by 3 and 5 by 5 COLOR scenes. In effect, the 7 by 7 filter minimized the noise in this COLOR scene, a consequence also noted in visual interpretation of the black-and-white imagery.

TABLE 1. ERRORS AND ACCURACY OF DENSITY SLICED SAR SCENES AT TWO SCALES

Scene	Omission Error (%)		Commission Error (%)		Accuracy %
	Urban	Non-Urban	Urban	Non-Urban	
CITY 3 × 3 Color	30.1	24.5	4.8	73.5	70.7
CITY 3 × 3 A	77.7	3.0	4.2	71.0	40.0
CITY 3 × 3 B	49.7	17.3	10.1	64.7	58.3
CITY 3 × 3 C	19.4	50.3	17.0	54.4	73.0
CITY 5 × 5 Color	31.9	22.4	4.5	74.1	69.3
CITY 5 × 5 A	79.1	3.0	4.5	71.3	39.7
CITY 5 × 5 B	52.9	13.9	8.8	65.2	56.8
CITY 5 × 5 C	24.9	40.4	15.0	56.0	71.3
CITY 7 × 7 Color	30.0	21.4	4.2	72.7	71.1
CITY 7 × 7 A	65.5	4.9	4.5	67.8	49.4
CITY 7 × 7 B	43.4	17.5	9.2	61.6	63.0
CITY 7 × 7 C	14.6	52.6	16.8	48.4	76.0
OVW 3 × 3 Color	46.6	16.5	17.4	45.0	65.6
OVW 3 × 3 A	90.5	1.3	14.5	43.0	58.4
OVW 3 × 3 B	60.2	26.8	45.0	40.3	58.1
OVW 3 × 3 C	25.0	70.4	53.3	41.0	50.1
OVW 5 × 5 Color	58.0	10.5	14.6	48.7	61.3
OVW 5 × 5 A	91.9	1.3	16.7	43.4	57.8
OVW 5 × 5 B	59.1	29.4	46.6	40.8	57.2
OVW 5 × 5 C	34.7	57.5	51.7	40.2	52.8
OVW 7 × 7 Color	40.3	19.2	18.0	42.2	68.2
OVW 7 × 7 A	80.6	5.2	24.4	41.1	60.8
OVW 7 × 7 B	51.6	37.6	48.5	40.4	56.1
OVW 7 × 7 C	30.4	64.3	52.9	41.2	51.0

Note: Color = visually interpreted color-coded scene;
  A indicates that the three highest response value density slices were designated as urban;
  B the four highest; and
  C the five highest.
  3 × 3, 5 × 5, 7 × 7 refer to the pixel filter used in generating the image.

When the COLOR scenes were classified solely by density slice, the most accurate results for all three filtered images at the CITY (maximum enlargement) scale were generated when the five highest signal response value density slices were designated as urban (i.e., 3 by 3C, 5 by 5C, 7 by 7C) and the two lowest levels as non-urban. In other words, the broadest range of signal response was used to define urban land cover. In contrast, for the OVW COLOR data groupings (smaller scale) the best results were found to be the scenes where the most narrow definition of urban (A) was used. Because the area of the CITY scenes included only the built-up area and immediate urban fringe, it is believed the broader response range in that instance allowed inclusion of the low return from residential areas. With the OVW COLOR scenes the larger study area (smaller scale) included many small exurban developments and suburban communities as well. Thus, the more restricted (higher response value) definition of urban land cover avoided confusion and overlap between the lower signal response of residential vegetation (urban) and the fields, pastures, forests, and woodland comprising non-urban land cover.

Overall, the best results (76 percent accuracy) of all the density-sliced data, visual/manual and semi-automated (breakpoint) interpretation, were produced using the 7 by 7 pixel filter of the large scale (CITY) image and an urban/non-urban land-cover breakpoint (C) that defined the five highest density slices as urban (i.e., 255-24).

LAND COVER MIX; The last phase of this study involved the examination of the mix of land cover types contained in each of the seven density slices and the range of brightness levels within each land-cover type (i.e., the homogeneity/heterogeneity of each land-cover type in terms of its radar signal response and vice versa). In examining and compiling these data, it was noted that the two lowest brightness levels (density slices) were mainly located in the non-built up and rural areas around the city. Because they seemed to have little relation to man-made cultural targets, these two slices were combined and defined as non-urban during data collection.

Although analysis was completed for the three CITY scale color-coded scenes and the three OVW scale color-coded scenes, for brevity only the results for the 3 by 3 filter CITY scene will be used as a basis for discussion. This scene was the most accurate of the six density-sliced, filtered, color-coded images and, consequently, represently the best data of the scenes examined.

The mix of signal response within each land-cover type for this image is indicated in Figure 1. It is apparent that each category is quite heterogeneous in respect to response levels. For example, cover type 11 (Residential) covered about 44 percent of the study area. Less than one percent (0.59) of this land cover produced the highest response of level 1, but 11.98 percent of the residential areas was at level 2, 13.66 percent at level 3, 26.83 at level 4, 32.48 percent at level 5, and 14.46 percent at level
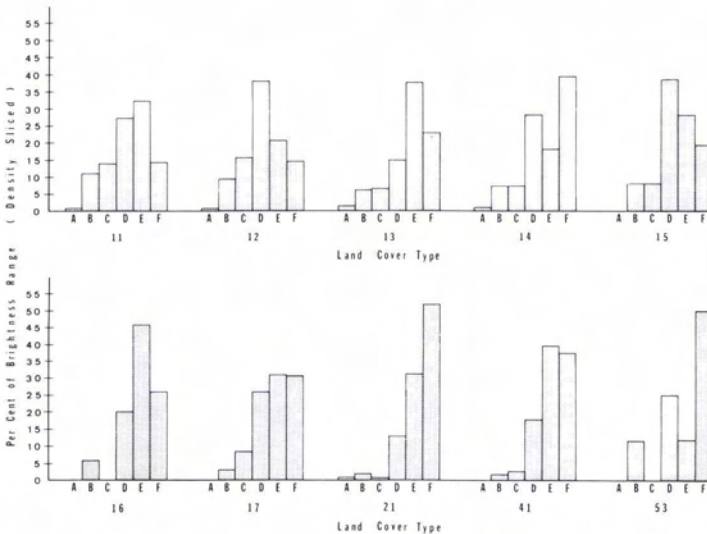

FIG. 1.   Percent of density slice (brightness range in each land-cover type for a 3 by 3 filter CITY scene. Land-cover type key and percent of total area: (11) residential (43.99%); (12) commercial and services (8.45%); (13) industrial (7.84%); (14) transportation, communications, and utilities (8.45%); (15) industrial and commercial complexes (1.26%); (16) mixed urban or built-up land (1.31%); (17) other urban or built-up land (4.01%); (21) cropland and pasture (20.08%); (41) deciduous forest land (4.27%); (53) reservoirs (0.35%). Density slice (brightness) ranges and percent of total area: (A) 255-121 (0.61%); (B) 120-80 (7.84%); (C) 79-50 (9.06%); (D) 49-34 (24.65%); (E) 33-24 (30.92%); (F) 23-1 (26.92%).

6. Similar distributions characterize the remaining cover types. Only in the broadest sense was any land-cover/density-slice relationship noticeable. Cover types with an extensive vegetation component (i.e., categories 16, 17, 21, 41, and 53) tended to be associated with lower response levels. Land cover containing buildings, structures, and related hard, cultural, man-made features (e.g., cover categories 11-15) did evidence a slight shift to higher brightness levels, but the distribution of such cover type's areas by density slice was still quite varied. For example, those categories with a large areal component of vegetation and/or plane surfaces as well as some structures (i.e., Residential (11); Industrial (13); and Transportation, Communications, and Utilities (14) were characterized by responses across the brightness range.

Another way of examining these data is provided in Figure 2. In this instance the composition of each density slice (according to land cover) is depicted. For example, the area with the brightest signal response (density slice A) was 42.86 percent Residential; 7.14 percent Commercial and Services (12); 21.43 percent Industrial (13); and so on. Again, the major observations pertain to the extreme heterogeneity of the residential land cover and the relationship between vegetation cover, man-made cultural targets, and strength of signal return. Residential land cover comprised the major portion of the response in all but the lowest brightness range. One might have expected that high returns would tend to be associated with land-cover types comprised of vertical surfaces, corner reflectors, and little vegetation (e.g., Commercial and Services, Industrial). This was obviously not the case as each range contained diverse land-cover types. At best,

only a very slight association is discernable between higher brightness levels and urban land cover and between lower response levels and non-urban/non-built-up areas. Both Figures 1 and 2 indicate that there is little correlation between a land-cover type and its radar signal response manifest as a density-sliced image of brightness levels.

SUMMARY AND DISCCUSION

Selected preprocessing techniques and interpretation approaches and the relationship between brightness levels and land-cover types have been examined with regard to the utility of digitally processed L-Band synthetic aperture radar imagery for urban land-cover mapping. Thirty-three distinct images generated from the original data of the 100 km by 100 km Seasat SAR scene served as the study base. These images consisted of data that had been processed at two enlargements, subjected to linear contrast stretch, averaged by three different pixel filter windows, and/or density sliced.

The most accurate and facile identification of urban and non-urban land cover was made from a black-and-white image that had undergone linear contrast stretch and maximum enlargement without resampling the data. Other manual interpretations of black-and-white and color-coded density-sliced imagery were less expedient and precise. An iterative, stepped procedure to define urban and non-urban land cover based solely on brightness levels was also less successful than the subjective, manual classification of the maximum enlargement black-and-white stretched image.

A comparison of land-cover type with the various density-sliced images indicated that little homogeneity existed between a land-cover class and its
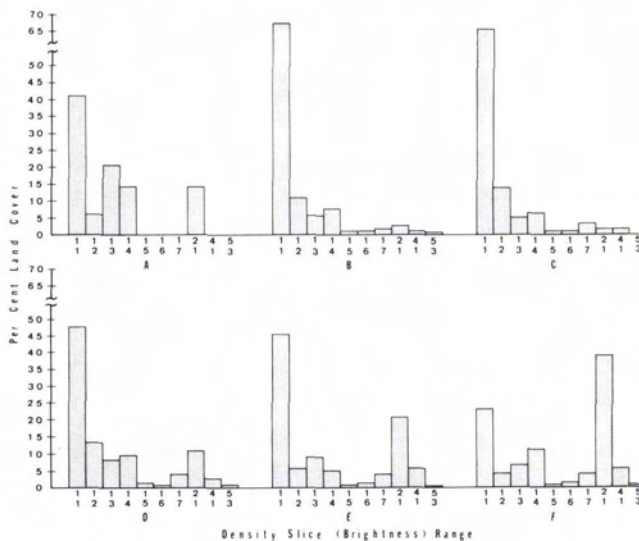

FIG. 2. Percent of land-cover type within each density slice (brightness range) for a 3 by 3 filter CITY scene. (See Figure 1 caption for the definition of land-cover types and density-slice range.)

radar return. As expected, higher returns were most prevalent among commercial and industrial land-cover concentrations while lower returns were associated with open land, pasture, forest, and cropland. However, no land-cover class could consistently be associated with a particular level slice. Although some within-land cover-class variation was anticipated, it was felt that by filtering and iteratively defining ranges or levels of return it might be possible to detect some Level II or modified Level II land-cover classes. Such was not the case. For example, residential land cover was found as a component of every level slice from the lowest to highest.

An explanation for this inability to identify detailed classes of land cover and limited success in delimiting the urban/non-urban land cover involves a combination of environmental and radar parameters. Perhaps the most pervasive influence is that exerted by the vegetation canopy and horizontal plane surfaces within and outside of the urban area. By concealing much if not all of the underlying structures, the mature trees presented either a uniform surface or a mixed, convoluted radar return. Horizontal plane surfaces such as grass, parking lots, and vacant land often comprised the major proportion of a land-cover surface. The return from these surfaces alone or in combination with the return from vegetation frequently dominated that from structures. Consequently, the return from low-density residential areas on the urban fringe was indistinct from that of adjacent crops and pasture, woodland and brush, and other non-urban land cover. The combination of vegetation and horizontal plane surfaces blurred the urban/non-urban interface as well as obfuscating the urban land-cover classes. This is readily apparent in examining the range of radar return for each land-cover type and the range of land covers within each density slice.

The effects of vegetation and horizontal plane surface were compounded by the nature of the land cover. Residential, commercial and service, industrial, and transportation land cover were not contiguous but fragmented and dispersed throughout the built-up area. Structures tended to be small, and lacked uniformity in size, orientation, shape, and spatial pattern. The result was a mixture of juxtaposed land covers whose individual elements (1) were individually less than the resolution of the SAR system, and (2) frequently contained as much within-class as between-class variation. Thus, from the perspective of the environment this might be considered a worst case scenario of what can be expected when using a single SAR image to define urban and non-urban land cover.

That texture remains an important, if imprecise, component of SAR image analysis is evident when the results of window filtering and scale enlargement are examined. The radar analyst relies on contextual and textural elements in defining land cover.

Texture differences were much more apparent on the large scale images than at the small scale. There was more image texture on the 3 by 3 filtered image than on the 5 by 5 or 7 by 7 filtered image. Concomitantly, the removal of texture removed contextual information from the image that the analyst used in discriminating cover type. Increasingly, there remained only tone on which to base decisions. The results of such a process indicate that tone alone is not sufficient if one wishes to identify urban land cover from radar imagery. However, how much texture should be present or removed is also a problem. The way in which texture contributed to interpretation accuracy was a function of the image, filter, and scale combination employed.

With regard to SAR system parameters, the results of this study lend further empirical evidence for the need to explore the potential advantages of employing multi-frequency, multi-polarized, and/or multi-look direction imagery. The benefits of such a multi-approach have been previously reported by Bryan (1975, 1979, 1981), Henderson (1979, 1980), Drake and Schuman (1974), and Waite et al. (1978, 1980).

REFERENCES

Anderson, J. R., E. E. Hardy, J. T. Roach, and R. E. Witmer, 1976. *A Land Use and Land Cover Classification System for use with Remote Sensor Data*, Geological Survey Professional Paper 964, U.S. Department of Interior, U.S. Government Printing Office, Washington, D.C. 28 p.

Bryan, M. L., 1975. Interpretation of an Urban Scene Using Multi-Channel Radar Imagery, *Remote Sensing of Environment*, Vol. 4, No. 1, pp. 49–66.

———, 1979. The Effect of Radar Azimuth Angle on Cultural Data, *Photogrammetric Engineering and Remote Sensing*, Vol. 45, No. 8, pp. 1097–1107.

———, 1981. Potentials for Change Detection Using Seasat Synthetic Aperture Radar Data, paper presented at the Institute of Electrical and Electronics Engineers 1981 International Geoscience and Remote Sensing Symposium, 8–10 June, Washington, D.C.

Drake, B., and R. A. Schuchman, 1974. Feasibility of Using Multiplexed SLAR Imagery for Water Resources Management and Mapping Vegetation Communities, *Proceedings of 9th International Symposium on Remote Sensing of Environment*, University of Michigan, Ann Arbor, pp. 219–231.

ESL, 1980. *Electromagnetic Systems Laboratory: IDIMS Functional Guide*, Vol. 1, Technical Manual ESL-TM705, Sunnyvale, California.

Estes, J. E., and L. W. Senger, 1971. An Electronic Multi-Image Processor, *Photogrammetric Engineering*, Vol. 37, No. 6, pp. 577–586.

Henderson, F. M., 1979. Land Use Analysis of Radar-Imagery, *Photogrammetric Engineering and Remote Sensing*, Vol. 45, No. 3, pp. 295–307.

————, 1980. Extracting Urban Data from Seasat SAR Imagery: The Merit of Image Enlargement and Density Slicing, *International Archives of Photogrammetry*, Vol. 23, Part B7, Commission VII (F. Ackerman, ed.), pp. 411–421.

Henderson, F. M., and S. W. Wharton, 1980. Seasat SAR Identification of Dry Climate Urban Land Cover, *International Journal of Remote Sensing*, Vol. 1, No. 3, pp. 293–304.

Waite, W. P., H. C. MacDonald, D. N. Tolman, C. A. Barlow, and M. Borengasser, 1978. Dual Polarized Long Wavelength Radar for Discrimination of Agricultural Land Use, *Proceedings of the American So-ciety of Photogrammetry Fall Technical Meeting*, Albuquerque, N.M., pp. 595–607.

Waite, W. P., H. C. MacDonald, J. S. Demarcke, and B. H. Corbell, 1980. Look Direction Dependence of Radar Backscattering Cross-Section for Agricultural Fields, *American Society of Photogrammetry Technical Papers*, Fall Meeting, Niagara Falls, New York, RS2G1-RS2G14.

Wharton, S. W., and F. M. Henderson, 1982. An Overview of the Characteristics of SEASAT SAR Data and Its Application to Urban Land-Cover Analysis in the Northeastern United States, *Journal of Applied Photographic Engineering*, Vol. 8, No. 1, pp. 63–67.

THE PHOTOGRAMMETRIC SOCIETY, LONDON

Membership of the Society entitles you to *The Photogrammetric Record* which is published twice yearly and is an internationally respected journal of great value to the practicing photogrammetrist. The Photogrammetric Society now offers a simplified form of membership to those who are already members of the American Society.

- -

APPLICATION FORM

PLEASE USE BLOCK LETTERS

To: The Hon. Secretary,
The Photogrammetric Society,
Dept. of Photogrammetry & Surveying
University College London
Gower Street
London WC1E 6BT, England

I apply for membership of the Photogrammetric Society as,
☐ Member — Annual Subscription — $26.00
☐ Junior (under 25) Member — Annual Subscription — $13.00
☐ Corporate Member — Annual Subscription — $156.00

(Due on application and thereafter on July 1 of each year.)

(The first subscription of members elected after the 1st of January in any year is reduced by half.)
I confirm my wish to further the objects and interests of the Society and to abide by the Constitution and By-Laws. I enclose my subscription.

Surname, First Names ....
Age next birthday (if under 25) ....
Profession or Occupation ....
Educational Status ....
Present Employment ....
Address

....

ASP Membership ....
Card No. ....

Signature of
Date .... Applicant...

Applications for Corporate Membership, which is open to Universities, Manufacturers and Operating Companies, should be made by separate letter giving brief information of the Organisation's interest in photogrammetry.